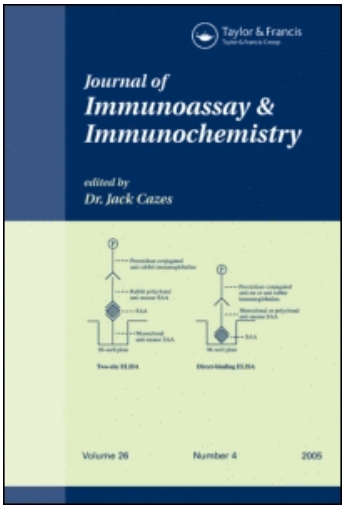

Journal of Immunoassay and Immunochemistry

Publication details, including instructions for authors and subscription information:
http://www.informaworld.com/smpp/title~content=t713597271

Kinetics of Androstendione-Radioactive Immunocomplex Substitution Reaction

R. Díez Montoro[a]; M. T. Salabert Salvador[a]; J. L. Moreno Frigols[a]
[a] Department of Physical Chemistry, Faculty of Pharmacy, Valencia, Spain

To cite this Article Montoro, R. Díez , Salvador, M. T. Salabert and Frigols, J. L. Moreno(2005) 'Kinetics of Androstendione-Radioactive Immunocomplex Substitution Reaction', Journal of Immunoassay and Immunochemistry, 26: 2, 97 — 107
To link to this Article: DOI: 10.1081/IAS-200051992
URL: http://dx.doi.org/10.1081/IAS-200051992

Journal of Immunoassay & Immunochemistry, 26: 97–107, 2005

ISSN 1532-1819 print/1532-4230 online
DOI: 10.1081/IAS-200051992

Kinetics of Androstendione-Radioactive Immunocomplex Substitution Reaction

R. Díez Montoro, M. T. Salabert Salvador, and J. L. Moreno Frigols
Department of Physical Chemistry, Faculty of Pharmacy, Valencia, Spain

Abstract: A kinetic model is put forward for the study of the antigen-antibody reactions involved in the coated tube radioimmunoassay (RIA) of androstendione. Twenty experiments were conducted to determine the influence of initial concentrations, ionic strength, viscosity, and temperature on the substitution reaction of ^{125}I-androstendione (M) by unlabelled androstendione (Q) in the immunocomplex PM (P = anti-androstendione antibody). The results obtained are in line with the proposed model. The concentration of radioactive immunocomplex is directly proportional to the initial concentration of labelled androstendione and independent of the concentration of unlabelled androstendione, ionic strength, and viscosity. The reaction is not diffusion-controlled.

Keywords: Kinetics, RIA, Substitution reaction, Androstendione

INTRODUCTION

Radioimmunoassay (RIA) is used for androstendione assessment. It is a competitive technique in which the antigen molecule to be determined (Ag) competes with a radioactive tracer (labelled antigen: Ag*) in order to bind to a specific antibody (Ab) that reacts to both antigens until equilibrium is reached for both immunocomplexes, i.e., the radioactive one and the non-radioactive or "cold" one- to coexist:[1]

$$\mathrm{Ag} + \mathrm{Ab} + \mathrm{Ag}^* \Longleftrightarrow (\mathrm{Ag} - \mathrm{Ab}) + (\mathrm{Ag} - \mathrm{Ab})^*$$

Address correspondence to Dr. José Luis Moreno Frigols, Departmento Química Física, Facultad de Farmacia, Avda. Vicent Estellés s/n, Burjassot 46100, Valencia, Spain. E-mail: jose.1.moreno@uv.es

By keeping tracer (Ag*) and antibody (Ab) quantities constant, the higher or lower proportion in the immunocomplexes formed will solely depend on the amount of cold antigen (Ag) in the sample to be analysed.

If the tracer behaves similarly when bound as when not bound, then the separation of the bound and free fractions is essential. In the technique observed in this research, separation is accomplished by fixation onto a second antibody coated on a plastic bead.

Kinetics and equilibrium in antigen-antibody reactions are determining factors of the rapidity, analytical range, and reliability[2] of immunoanalytical techniques. Likewise, the search for more reliable, faster immunoassays is one of the main development areas in this field. This has caused the overall process to be progressively automated, from sample handling to statistical assessment of results. Yet, despite the large number of immunoanalytical systems developed in recent years, very few of them include kinetic analysis.

Several models have been proposed for the fitting of kinetic data in association and disassociation reactions.[3,4]

Through continuous flow immunoassays, Rabbany et al.[5] analysed the dissociation kinetics of the labelled antigen—immobilised antibody complex in the absence of unlabelled antigen. In another paper, Rabbany et al.[6] studied displacement kinetics for an immunoassay in trinitrotoluene (TNT) continuous flow against its antigen immobilised on a porous membrane. The latter assay type suggests that lower flow rates produce a longer interaction between the injected unlabelled antigen and the labelled antigen-antibody complex and, consequently, a greater labelled antigen displacement, with more intense signals being recorded.

Velge-Roussel[7] completed several analyses using biosensor techniques to determine kinetic and thermodynamic parameters in the interaction between surface proteins in CD4 cells and one of the antibodies inhibiting the first stage of HIV arrival in the host cell. Data obtained by a non-linear regression method were analysed they produced a bi-exponential curve.

Andersson et al.[8] used a BIACORE system to measure kinetic parameters in the reaction between Fab57P and 18 peptides, analogous to an epitope of the tobacco mosaic virus protein, at several pH values and in the presence of different additives (NaCl, urea, EDTA, KSCN, and DMSO). They developed mathematical models with good predictive power. Urea, DMSO, and NaCl had an effect on the bonding, while pH changes and the presence of EDTA and KSCN produced no effects.

In our previous research,[9–15] various features relative to the kinetics of antigen-antibody reactions used by immunoanalytical techniques were analysed. Theoretical models were prepared for an application to the immunocomplex formation processes produced in RIA (radioimmunoassay) and IRMA (immunoradiometric assay). We also studied the fitting of equilibrium results to several pre-set equations, and a mathematical deduction that justifies them theoretically was obtained.

In line with the above research, this paper aims to:

- Produce a new kinetic model that is applicable to the substitution of the labelled antigen bound to the antibody by the unlabelled one, this process being at the foundations of RIA.
- Determine potential diffusion control.

This must be done in different stages:

- Obtaining integrated rate equations for the overall processes.
- Studying the medium's temperature and viscosity influence on reaction kinetics.
- Complementary analysis of ionic strength influence in order to include or rule out the effect of electrical charges.

EXPERIMENTAL

Instruments

ILKB Gammamaster Automatic Gamma Counter. Brookfield DV–II digital viscosimeter. Viscosity measurements were performed at 60 rpm with a UL adapter at room temperature.

Reagents

DM: Solution of ^{125}I-labelled androstendione in a protein-based buffer.
PT: Plastic tubes with rabbit anti-androstendione immunoglobulin immobilized to the inside wall.
DQ: Androstendione standard solutions.

These reagents were included in the androstendione RIA DSL-3800 kit.

GL: Glycerol, Merck pro analysis.
DS: Solution of NaCl, 2.05 M.

Several tube series were prepared as per the following table:

PT	1–6	7–12	13–18	19–120
DM (mL)	0.25	0.50	0.75	1
H_2O (mL)	0.75	0.50	0.25	0

They were left to react overnight. The next day, they were decanted and washed with 2 mL distilled water.

Solutions were prepared containing:

Solution	1	2	3	4	5	6	7	8	9	10
DQ (μL)	25	50	75	100	100	100	100	100	100	800
GL (mL)	0	0	0	1	2	3	0	0	0	0
DS (μL)	100	100	100	100	100	100	200	300	400	800
H_2O (mL)	7.875	7.850	7.825	6.8	5.8	4.8	7.7	7.6	7.5	62.4

Experimental Procedure

Activity was measured for tubes 1, 2, 3, and 4 at 0 minutes using a gamma counter. Reaction kinetics were studied by placing 1 mL of the previously mentioned solutions into the plastic coated tubes and letting them react at different times and at 48 hours, this being considered infinite time. Each tube was washed to remove any unbound labelled antibody. Any radioactivity present in the remaining bound labelled antibody was then measured using a gamma counter.

Twenty experiments were performed, arranged as follows:

Experiments 1–4

Study of the influence of ^{125}I-androstendione concentration (m) upon the global reaction using tubes 1–24 and solution 10.

Experiments 5–8

Study of the influence of androstendione concentration (q) and temperature (T) upon the global reaction using tubes 25–48 and solutions 1, 2, 3, and 10.

Experiments 9–12

Study of the influence of ionic strength (I), using tubes 49–72 and solutions 7, 8, 9, and 10.

Experiments 13–16

Study of the influence of viscosity (η) using tubes 73–96 and solutions 4, 5, 6, and 10. The final viscosities of the solutions obtained in this manner were determined by comparison with a calibration curve drawn from standard glycerol–water mixtures.

Experiments 17–20

Study of the influence of temperature (T) using tubes 96–120 and solution 10.

Data Analysis

The Statistica programme (Copyright © StatSoft, Inc., 1993) was used with specific non-linear regression equations. As the statistical criterion[16,17] that allows a choice from different equations, SS and Corrected Akaike's Information Criterion (AIC_c) was used, expressed as

$$AIC_C = N \cdot \ln\left(\frac{SS}{N}\right) + 2P + \frac{2p(p+1)}{N - p - 1}$$

where N is the number of points, SS the addition of residual squares, and p the number of parameters in the equation. The fitting with the lowest AIC_c must be chosen. In order to distinguish equations from monoexponential and biexponential models, AICc and ANOVA (F-test) were used.

THEORETICAL MODEL

This is the reaction studied:

$$PM + Q \longleftrightarrow PQ + M$$

P = Anti-androstendione antibody immobilised on the tube wall, M = ^{125}I-androstendione, PM = radioactive immunocomplex, Q = androstendione, and PQ = non-radioactive immunocomplex.

Using these symbols:

$$(PM)_0 = m; \quad (Q)_0 = q; \quad (PM) = m - x;$$
$$(Q) = q - x; \quad (PQ) = (M) = x$$
$$k_1 = \text{direct rate constant}; \quad k_2 = \text{reverse rate constant}.$$

then:

$$dx/dt = k_1(m - x)(q - x) - k_2x^2 \tag{1}$$

This must be true at equilibrium:

$$0 = k_1(m - x_e)(q - x_e) - k_2x_e^2 \tag{2}$$

From (1) and (2) we have:

$$dx/dt = (k_1 - k_2)(x_e - x)[(mqk_1/(k_1 - k_2)x_e) - x] \tag{3}$$

By integrating (3) we have:

$$x = x_e\{1 - \exp(-tk_1(2mq/x_e - m - q))\}/\{1 - [x_e^2(k_1 - k_2)/(mqk_1)] \times \exp(-tk_1(2mq/x_e - m - q))\} \quad (4)$$

Our experiments measured PM activity, represented by z, directly proportional to (PM). Therefore:

$$z_0/m = (z_0 - z)/x = (z_0 - z_e)/x_e = C \quad (5)$$

Taking into account that:

$$1 - [x_e^2(k_1 - k_2)/(mqk_1)]\exp(-tk_1(2mq/x_e - m - q)) \approx 1 \quad (6)$$

From (4), (5), and (6) we obtain:

$$z = z_e + (z_0 - z_e) \cdot \exp\{-tk[2z_0Cq/(z_0 - z_e) - z_0 - Cq]\} \quad (7)$$

$$\begin{aligned} 2z_0Cq/(z_0 - z_e) - z_0 - Cq &= (2z_0Cq - z_0^2 - z_0Cq + z_0z_e + Cqz_e)/(z_0 - z_e) \\ &= z_0(Cq + z_e - z_0)/(z_0 - z_e) + Cqz_e/(z_0 - z_e) \\ &= z_0(Cq/(z_0 - z_e) - 1) + Cqz_e/(z_0 - z_e) \\ &= a'z_0 + b = a'Cm + b = am + b \end{aligned} \quad (8)$$

$$\begin{aligned} k_1/k_2 = K &= (PQ)(M)/(PM)(Q) \\ &= c \cdot \exp(-\Delta H^0/RT)(\text{van t'Hoff}) \end{aligned} \quad (9)$$

$$\begin{aligned} q = (Q) + (PQ) &= (Q) + K(PM)(Q)/(M) \approx K(PM)(Q)/(M) \\ &= Kz_e(Q)/(z_0 - z_e) \end{aligned} \quad (10)$$

$$z_e = qz_0/(q + K(Q)) \approx qz_0/K(Q) = qz_0/[(Q) \cdot c \cdot \exp(-B/T)] \quad (11)$$

$$k = d \cdot T\exp(-\Delta H^{\neq}/T) \text{ (Eyring)} \quad (12)$$

From (5), (7), (8), (9), (10), (11), and (12), we have:

$$z = A \cdot m \cdot \exp(B/T) + [C \cdot m - A \cdot m \cdot \exp(B/T)] \times \exp[-t \cdot (D \cdot m + E) \cdot T \cdot \exp(-F/T)] \quad (13)$$

RESULTS AND DISCUSSION

Results are shown in Table 1.

Table 1. z values for experiments 1–20

t (min)	0	12	24	36	48	60	Infinite	m	q	I	η	T (K)
z_1	3991.5	2373.0	1627.0	1272.44	1077.7	993.8	771.9	25	100	0.0256	1.385	318
z_2	7906.9	3750.2	2982.6	2270.8	2162.0	1887.0	1534.9	50	100	0.0256	1.385	318
z_3	12253.0	5391.6	3839.0	3085.0	2638.4	2552.7	2446.3	75	100	0.0256	1.385	318
z_4	15191.8	6816.1	4498.1	3808.9	3506.9	3393.9	3192.0	100	100	0.0256	1.385	318
z_5	15191.8	9434.0	7430.9	6731.2	6406.4	6285.9	4440.8	100	25	0.0256	1.385	308
z_6	15191.8	9274.9	7906.0	7360.9	6918.0	6675.0	—	100	50	0.0256	1.385	308
z_7	15191.8	8926.9	7660.9	6822.4	6652.5	6095.3	—	100	75	0.0256	1.385	308
z_8	15191.8	6816.1	4498.1	3808.9	3506.9	3393.9	3192.0	100	100	0.0256	1.385	318
z_9	15191.8	6816.1	4498.1	3808.9	3506.9	3393.9	3192.0	100	100	0.0256	1.385	318
z_{10}	15191.8	7660.3	5429.0	4257.0	3661.2	3479.3	—	100	100	0.0513	1.385	318
z_{11}	15191.8	7214.4	5127.4	3910.2	3551.9	3886.4	3315.0	100	100	0.0769	1.385	318
z_{12}	15191.8	7406.0	4868.0	4093.5	3355.7	2894.0	—	100	100	0.1026	1.385	318
z_{13}	15191.8	6816.1	4498.1	3808.9	3506.9	3393.9	3192.0	100	100	0.0256	1.385	318
z_{14}	15191.8	6591.2	4902.0	3659.3	3300.0	2975.0	—	100	100	0.0256	1.478	318
z_{15}	15191.8	6373.3	4383.2	3424.2	2999.6	2305.1	—	100	100	0.0256	1.677	318
z_{16}	15191.8	6709.4	4394.0	3406.0	2667.9	2440.5	—	100	100	0.0256	1.980	318
z_{17}	15191.8	6816.1	4498.1	3808.9	3506.9	3393.9	3192.0	100	100	0.0256	1.385	318
z_{18}	15191.8	10530.0	8950.7	7569.0	7199.2	6662.6	4176.8	100	100	0.0256	1.385	308
z_{19}	15191.8	11344.0	11252.2	10576.6	10837.0	9846.0	5476.4	100	100	0.0256	1.385	300
z_{20}	15191.8	12924.9	11903.9	11788.4	11101.3	11016.0	8602.4	100	100	0.0256	1.385	293

z = Activity (cpm) of PM immunocomplex. The subscript indicates the experience number.
m = PM initial concentration (relative units).
I = Ionic strength ($mol \cdot L^{-1}$).
η = Viscosity ($mPa \cdot s$).
T = Temperature (K).
q = Q initial concentration (relative units).

Influence of m (Experiments 1–4)

The results of experiments 1–4 are fitted to the equation:

$$z = 34.4 \cdot m + (156.0 \cdot m - 34.4 \cdot m) \times \exp(-t \cdot (0.000634 \cdot m + 0.0431)) \quad (14)$$

$$r = 0.998; \quad SS = 1.161 \cdot 10^{-6}$$

Equation (14) has the following form:

$$z = A_1 \cdot m + (C \cdot m - A_1 \cdot m\cdot) \cdot \exp(-t \cdot (D_1 \cdot m + E_1))$$

It is obtained by making T constant in (13). It shows that the initially obtained z values and the values at equilibrium are directly proportional to m. The apparent rate constant is a linear function of m, which suggests ^{125}I-androstendione is in excess with regard to androstendione.

Influence of q and T (Experiments 5–8)

The results of experiments 5–8 are fitted to the equation:

$$z = 2.18 \cdot 10^{-5} \cdot \exp(5996/T) + (15131 - 2.18 \cdot 10^{-5} \cdot \exp(5996/T)) \times \exp(-t \cdot T \cdot (12.64 + 117.5 \cdot 10^{-4} \cdot q) \cdot \exp(-1566/T)) \quad (15)$$

$$r = 0.993; \quad SS = 4.96 \cdot 10^{6}; \quad AICc = 336.3$$

which is obtained by making m constant in (13), remembering that q is included in parameter E. Equation (15) can be simplified to:

$$z = 2.533 \cdot 10^{-6} \cdot \exp(6666/T) + (15145 - 2.533 \cdot 10^{-6} \cdot \exp(6666T)) \times \exp(-t \cdot T \cdot 0.0896) \quad (16)$$

$$r = 0.992; \quad SS = 5.27 \cdot 10^{6}; \quad AICc = 330.7$$

Equation (16) is preferable to (15), as it provides a lower AICc value. This shows process kinetics to be apparently independent from q.

Influence of I (Experiments 9–12)

The results of experiments 9–12 are fitted to the equation:

$$z = 3411 + (15163 - 3411) \cdot \exp(-t \cdot 0.1036 \cdot \exp(-0.603 \cdot I^{0.5})) \quad (17)$$

$$r = 0.998; \quad SS = 1.76 \cdot 10^{6}; \quad AICc = 302.2$$

which is obtained by making m and T constant in (13), introducing the Debye-Hückel expression in D, and assuming E to be negligible. Equation (17) can be simplified to:

$$z = 3412 + (15162 - 3412) \cdot \exp(-t \cdot 0.0893) \tag{18}$$
$$r = 0.998; \quad SS = 1.92 \cdot 10^6; \quad AICc = 301.4$$

Equation (18) is preferable to (17), as it provides a lower AICc value. This shows process kinetics to be apparently independent of I.

Influence of η (Experiments 13–16)

The results of experiments 13–16 are fitted to the equation

$$z = 3027 + (15153 - 3027) \cdot \exp(-t \cdot 0.0789/(1 - 0.109 \cdot \eta)) \tag{19}$$
$$r = 0.997; \quad SS = 2.52 \cdot 10^6; \quad AICc = 238.73$$

Kramers[18] proposed:

$$k_0/k_v = A' + B'\eta/\eta_0$$

where k_0 and k_v represent the rate constants corresponding to viscosities η_0 and $\tilde{\eta}$. Equation (19) is drawn from (13), making m and T constant and introducing Kramer's expression in D and assuming E to be negligible.

Equation (19) can be simplified to:

$$z = 3033 + (15155 - 3033)\exp(-t \cdot 0.0963) \tag{20}$$
$$r = 0.997; \quad SS = 2.52 \cdot 10^6; \quad AICc = 234.97$$

Equation (20) is preferable to (19) as it provides a lower AICc value. This shows process kinetics to be apparently independent of medium viscosity.

Influence of T (Experiments 17–20)

The results of experiments 17–20 are fitted to the equation:

$$z = (0.1326\exp(3224/T)) + (14370 - 0.1326\exp(3224/T))$$
$$\exp(-t \cdot 4.72 \cdot 10^8 T\exp(-7519/T)) \tag{21}$$
$$r = 0.982; \quad SS = 1.41 \cdot 10^6$$

Equation (21) is obtainewd from (13), making m constant and D negligible.

Experiments 1–20

The results are fitted to:

$$\begin{aligned} z = {} & 5.298 \cdot 10^{-4} m \cdot \exp(3519/T) + 149.5m - 5.298 \cdot 10^{-4} m \cdot \\ & \times \exp(3519/T)) \exp(-t \cdot (31026 + 3414m) \\ & \times T \exp(-6836/T)) \end{aligned} \tag{22}$$

$$r = 0.992; \quad SS = 3.96 \cdot 10^7$$

It is analogous to (13) and contains all the previous ones. From it we draw:

$$\Delta H^0 = 8.31 \cdot 3519 = 29243\,J \cdot mol^{-1}$$

$$\Delta H^{\neq} = 8.31 \cdot 6836 = 56807\,J \cdot mol^{-1}$$

CONCLUSIONS

- Theoretical model was prepared to study the kinetics of the substitution reaction in the immunocomplex antibody-labelled androstendione (PM) by unlabelled androstendione (Q).
- Equations linking PM concentration with time, M and Q concentrations, ionic strength, viscosity, and temperature were obtained.
- Experimental results were satisfactorily fitted to the theoretical model.
- The radioactive immunocomplex concentration is directly proportional to the initial concentration of androstendione at all times.
- The concentration of radioactive immunocomplex is apparently independent of the concentration of unlabelled androstendione, ionic strength, and viscosity.
- The radioactive immunocomplex concentration is temperature-dependent, as per Eyring and van't Hoff equations.
- The reaction is endothermic, $\Delta H^0 = 29243\,J \cdot mol^{-1}$
- Activation enthalpy is $H^{\neq} = 56807\,J \cdot mol^{-1}$, much higher than the viscous flow energy of water.
- The reaction is not diffusion-controlled.

REFERENCES

1. Yalow, R.S.; Berson, S.A. General aspects of radioimmunoassay procedures. In *In vitro procedures with radioisotopes in medicine*; Vienna, 1970; 455–481.
2. Zuber, E.; Mathis, G.; Flandrois, J.-P. Homogeneous two-site immunometric assay kinetics as a theoretical tool for data analysis. Anal. Biochem. **1997**, *25*, 79–88.
3. Zuber, E.; Rosso, L.; Darbouret, B.; Socquet, F.; Mathis, G.; Flandrois, J.P. A descriptive model for the kinetics of a homogeneous fluorometric immunoassay. J. Immunoassay **1997**, *18* (1), 21–47.

4. Rabbany, S.Y.; Piervicenzi, R.T.; Kusterbeck, A.W.; Bredehorst, R.; Ligler, F. Dissociation rate kinetics in a solid-phase flow immunoassay. Anal. Lett. **1998**, *31* (10), 1663–1675.
5. Rabbany, S.Y.; Marganski, W.A.; Kursterbeck, A.W.; Ligler, F.S. A membrane-based displacement flow immunoassay Biosens. Bioelectron. **1998**, *13* (9), 939–944.
6. Rabbany, S.Y.; Kursterbeck, A.W.; Bredehorst, R.; Ligler, F.S. Effect of antibody density on the displacement kinetics of a flow immunoassay. J. Immunol. Meth. **1994**, *168* (2), 227–234.
7. Velge-Roussel, F.; Breton, P.; Lescure, F.; Guillon, X.; Bout, D.; Hoebeke, J.J. Analysis of human CD4-antibody interaction using the BIAcore system. J. Immunol. Meth. **1995**, *183* (1), 141–148.
8. Andersson, K.; Choulier, L.; Hamalainen, M.D.; van Regenmortel, M.H.; Altschub, D.; Malmqvist, M. Predicting the kinetics of peptide-antibody interactions using a multivariate experimental design of sequence and chemical space. J. Molec. Recog. **2001**, *14* (1), 62–71.
9. Olivas, C.; Arroyo, C.; Moreno Frigols, J.L. Influence of viscosity and ionic strength on the reaction kinetics of aldosterone and androstendione and their specific antibodies. J. Pharm. Biomed. Anal. **2001**, *26* (4), 547–562.
10. Olivas Arroyo, C.; Duart Duart, M.J.; Moreno Frigols, J.L. Kinetics and equilibrium in insulin radioimmunoassay. J. Immunoassay Immunochem. **2002**, *23* (4), 407–428.
11. Duart Duart, M.J.; Olivas Arroyo, C.; Moreno Frigols, J.L. Validation of a kinetic model for the reactions in RIA. Clin. Chem. Lab. Med. **2002**, *40* (11), 1161–1167.
12. García Gómez, J.; Porcar Pons, M.; Moreno Frigols, J.L. Some kinetic aspects in the immunoradiometric assay of insulin-like growth factor binding protein-3. J. Pharm. Biomed. Anal. **2002**, *29*, 307–315.
13. García Gómez, J.; Moreno Frigols, J.L. Kinetics and equilibrium in the immunoradiometric assay (IRMA) of Thyroglobuline. J. Immunoassay Immunochem. **2002**, *23* (3), 347–367.
14. García Gómez, J.; Moreno Frigols, J.L. Comparison between mono- and bi-exponential models for reaction kinetics in the immunoradiometric assay of neuron-specific enolase. J. Pharm. Biomed. Anal. **2003**, *33*, 891–901.
15. García Gómez, J.; Moreno Frigols, J.L. A two-site model for reaction kinetics in the immunoradiometric assay (irma) of skeletal alkaline phosphatase (sALP). J. Immunoassay Immunochem. *accepted*.
16. Motulsky, H.J.; Cristopoulos, A. Fitting models to biological data using lineal and nonlineal regresion. In *A practical guide to curve fitting, GraphPad Software Inc: San Diego, CA, 2003; www.graphpad.com.*
17. Burnham, K.P.; Anderson, D.R. Model selection and multimodel interference. A practical information- theoretical approach. In , 2nd Ed.; Springer, 2002.
18. Kramers, H.A. Brownian motion in a field of force and the diffusion model of chemical reactions. Physica **1940**, *7*, 284–304.

Received November 26, 2004
Accepted December 24, 2004
Manuscript 3151